$Me_2CuLi*LiCN$ in Diethyl Ether Prefers a Homodimeric Core Structure $[Me_2CuLi]_2$ and Not a Heterodimeric One $[Me_2CuLi*LiCN]$: ^1H, ^6Li HOE and ^1H, ^1H NOE Studies by NMR

Ruth M. Gschwind,* Xiulan Xie, Pattuparambil R. Rajamohanan, Carsten Auel, and Gernot Boche

Contribution from the Fachbereich Chemie, Philipps-Universität Marburg, Hans-Meerwein-Strasse, D-35032 Marburg, Germany

Received December 27, 2000. Revised Manuscript Received April 3, 2001

Abstract: H−Li distances and $^1H-^1H$ dipolar interactions in $Me_2CuLi*LiCN$ and Me_2CuLi in diethyl ether (Et_2O), obtained by NMR spectroscopy, were used to gain structural information about the contact ion pair of the salt-containing organocuprate $Me_2CuLi*LiCN$ in this solvent. The H−Li distances of $Me_2CuLi*LiCN$ and Me_2CuLi in Et_2O, resulting from the initial buildup rates in conjunction with the motional correlation times, are almost identical, indicating a similar homodimeric core structure $[Me_2CuLi]_2$ for both samples. However, the H−Li distances obtained for $Me_2CuLi*LiCN$ do not rigorously exclude a heterodimeric structure [Me_2-CuLi*LiCN] as proposed by ab initio calculations. Therefore, $^1H-^1H$ dipolar interactions were investigated by SYM-BREAK-NOE/ROE-HSQC experiments, which allow for the observation of NOEs between equivalent protons. Since these experiments showed similar $^1H-^1H$ dipolar interactions of $Me_2CuLi*LiCN$ and Me_2-CuLi, we propose that for $Me_2CuLi*LiCN$ a homodimeric core structure $[Me_2CuLi]_2$ indeed is predominant in Et_2O.

Introduction

Despite the wide application of organocuprates in organic syntheses,[1] little is known about the structural details and aggregation states of these species in solution.[2a,b] Besides the recently solved question of "higher order" or "lower order" cyanocuprates,[2a,c,d] structures of organocuprates in solution are often derived from results of X-ray crystallography[3] and theoretical calculations.[4] Our recent NMR investigations have shown that organocuprates exist in an equilibrium between solvent separated ion pairs (SSIPs) and contact ion pairs (CIPs) in etheral solutions. They also indicate that the state of the equilibrium depends mostly on solvent properties.[3h,5] The assumption that CIPs represent the reactive species with enones is in excellent agreement with logarithmic reactivity profiles (LRPs) in diethyl ether (Et_2O) and tetrahydrofuran (THF)[3h,6] and with theoretical calculations performed for reactions of R_2CuLi and $R_2CuLi*LiCl$ with enones.[4f,g,i]

For salt-free Me_2CuLi (**1**) in Et_2O various studies (crystallographical studies of similar compounds,[3c,h] quantum chemical calculations[4b,d,f,g,i] and colligative measurements[7]) consistently indicate a homodimeric structure **I** (Figure 1). Therefore, we decided to use this system in our studies as a model of salt-free CIPs in solution.

$[H_3C—Cu—CH_3]^- Li^+$ **1** $\qquad$ $[H_3C—Cu—CH_3]^- Li^+*LiCN$ **1***LiCN

As a model for a salt-containing organocuprate in Et_2O the $Me_2CuLi*LiCN$ (**1***LiCN) system was chosen. However, con-

* To whom correspondence should be addressed. Phone: ++49 +6421 2825520. Fax: ++49 +6421 2828917. E-mail: ru@chemie.uni-marburg.de.

(1) (a) Lipshutz, B. H. *Organometallics in Synthesis*; Schlosser, M., Ed.; Wiley: Chichester, U.K., 1994; pp 283−382. (b) *Organocopper Reagents: A Practical Approach*; Taylor, R. J. K., Ed.; Oxford University Press: Oxford, U.K., 1994. (c) Krause, N. *Metallorganische Chemie*; Spektrum Akademischer Verlag: Heidelberg, Germany, 1996; pp 175−191.

(2) (a) Highlight: Krause, N. *Angew. Chem.* **1999**, *111*, 83−85. Krause, N. *Angew. Chem., Int. Ed. Engl.* **1999**, *38*, 79−81. (b) Bertz, S. H.; Dabbagh, G.; He, X.; Power, P. P. *J. Am. Chem. Soc.* **1993**, *115*, 11640−11641. (c) Bertz, S. H. *J. Am. Chem. Soc.* **1990**, *112*, 4031−4032. (d) Bertz, S. H. *J. Am. Chem. Soc.* **1991**, *113*, 5470−5471.

(3) (a) Eaborn, C.; Hitchcock, P. B.; Smith, J. D.; Sullivan, A. C. *J. Organomet. Chem.* **1984**, *263*, C23−C25. (b) Hope, H.; Olmstead, M. M.; Power, P. P.; Sandell, J.; Xu, X. *J. Am. Chem. Soc.* **1985**, *107*, 4337−4338. (c) Olmstead, M. M.; Power, P. P. *Organometallics* **1990**, *9*, 1720−1722. (d) Olmstead, M. M.; Power, P. P. *J. Am. Chem. Soc.* **1990**, *112*, 8008−8014. (e) Lorenzen, N. P.; Weiss, E. *Angew. Chem.* **1990**, *102*, 322−324; *Angew. Chem., Int. Ed. Engl.* **1990**, *29*, 300−302. (f) Kronenburg, C. M. P.; Jastrzebski, J. T. B. H.; Spek, A. L.; van Koten, G. *J. Am. Chem. Soc.* **1998**, *120*, 9688−9689. (g) Boche, G.; Bosold, F.; Marsch, M.; Harms, K. *Angew. Chem.* **1998**, *110*, 1779−1781; *Angew. Chem., Int. Ed. Engl.* **1998**, *37*, 1684−1686. (h) John, M.; Auel, C.; Behrens, C.; Marsch, M.; Harms, K.; Bosold, F.; Gschwind, R. M.; Rajamohanan, P. R.; Boche, G. *Chem. Eur. J.* **2000**, *6*, 3060−3068.

(4) (a) Snyder, J. P.; Spangler, D. P.; Behling, J. R. *J. Org. Chem.* **1994**, *59*, 2665−2667. (b) Böhme, M.; Frenking, G.; Reetz, M. T. *Organometallics* **1994**, *13*, 4237−4245. (c) Stemmler, T. L.; Barnhart, T. M.; Penner-Hahn, J. E.; Tucker, C. E.; Knochel, P.; Böhme, M.; Frenking, G. *J. Am. Chem. Soc.* **1995**, *117*, 12489−12497. (d) Bertz, S. H.; Vellekoop, A. S.; Smith, R. A. J.; Snyder, J. P. *Organometallics* **1995**, *14*, 1213−1220. (e) Snyder, J. P.; Bertz, S. H. *J. Org. Chem.* **1995**, *60*, 4312−4313. (f) Nakamura, E.; Mori, S.; Morokuma, K. *J. Am. Chem. Soc.* **1997**, *119*, 4900−4910. (g) Mori, S.; Nakamura, E. *Chem. Eur. J.* **1999**, *5*, 1534−1543. (h) Nakamura, E.; Yamanaka, M. *J. Am. Chem. Soc.* **1999**, *121*, 8941−8942. (i) Nakamura, E.; Mori, S. *Angew. Chem.* **2000**, *112*, 3902−3924; *Angew. Chem., Int. Ed. Engl.* **2000**, *39*, 3750−3771.

(5) Gschwind, R. M.; Rajamohanan, P. R.; John, M.; Boche, G. *Organometallics* **2000**, *19*, 2868−2873.

(6) (a) Bertz, S. H.; Eriksson, M.; Miao, G.; Snyder, J. P. *J. Am. Chem. Soc.* **1996**, *118*, 10906−10907. (b) Bertz, S. H.; Chopra, A.; Eriksson, M.; Ogle, C. A.; Seagle, P. *Chem. Eur. J.* **1999**, *5*, 2680−2691.

(7) (a) Gregory, C. D.; Pearson, R. G. *J. Am. Chem. Soc.* **1976**, *98*, 4098−4104. (b) Ashby, E. C.; Watkins, J. J. *J. Am. Chem. Soc.* **1977**, *99*, 5312−5317. (c) Gerold, A.; Jastrzebski, J. T. B. H.; Kronenburg, C. M. P.; Krause, N.; van Koten, G. *Angew. Chem.* **1997**, *109*, 778−780; *Angew. Chem., Int. Ed. Engl.* **1997**, *36*, 755−757 (THF!).

10.1021/ja004350x CCC: $20.00
Published on Web 07/10/2001

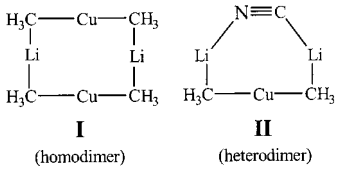

Figure 1. Schematic structures of a homodimer (**I**) and a representative of heterodimers (**II**).

trary to the results reported for Me_2CuLi (**1**) in Et_2O, the structure of the CIPs of salt-containing **1***LiCN represents a rather inconsistent picture. An extended X-ray absorption fine structure (EXAFS) study,[8] an infrared study in THF,[9] and most of the theoretical calculations[4a,c,e,i] indicate a heterodimeric structure **II** (Figure 1).

However, in compounds crystallized from solutions which contain LiX (X = Br, CN), the presence of a LiX salt was not observed, and a homodimer was obtained as the basic structural element.[3c,h] Based on ^{13}C chemical shifts and results of theoretical calculations performed for **1***LiI, an equilibrium between a homodimeric and a heterodimeric structure, with the homodimer as the main contributor, has been suggested.[4d] The analysis of ^{15}N chemical shifts of Bu_2CuLi*LiCN indicated the presence of structures containing a $LiCNLi^+$ unit. However, the relative positions between Bu_2Cu^- and $LiCNLi^+$ could not be defined.[10] Furthermore, our ^1H, ^6Li HOESY spectra showed small differences in the cross-peak intensities for both **1***LiCN and **1** in Et_2O.[3h] Thus, the structure of the CIPs of salt-containing organocuprates in solution, which are supposed to be the reactive species with enones,[3h,4i] is yet to be defined.

In this study we present the first application of the through space dipolar interactions (^1H, ^6Li HOE and ^1H, ^1H NOE) to derive structural information of salt-containing organocuprates in solution by NMR spectroscopy. Quantitative $^1H-^6Li$ dipolar interactions and qualitative $^1H-^1H$ dipolar interactions of the two model compounds **1***LiCN and **1** in Et_2O were used to asses whether salt-containing cuprates in Et_2O exist mainly in the form of a homodimer **I** or a heterodimer **II**. For the structural investigations a new pulse sequence, the SYM-BREAK-ROE-HSQC, was developed, which is based on the SYM-BREAK-NOE-HSQC.[11] These experiments allow for the detection of long-range NOEs/ROEs between equivalent protons even in the presence of additional relaxation sources such as quadrupolar nuclei.

Results and Discussion

^1H, ^6Li HOE Buildup Curves and H−Li Distances. Quantification of the differences in $^1H-^6Li$ dipolar interactions between **1***LiCN and **1** is one of the possible approaches for distinguishing between a heterodimeric (**II**) and a homodimeric structure (**I**) of **1***LiCN. In the case of a homodimer (**I**), 6 protons contribute to ^1H, ^6Li HOE, whereas for a heterodimer (**II**) 3 protons are involved in the HOE transfer (Figure 1). Therefore, a comparison of experimentally determined H−Li distances for **1***LiCN (calculated for 3 and 6 protons) and **1** (calculated for 6 protons) with the results of quantum chemical calculations should indicate the preference for **I** or **II**.

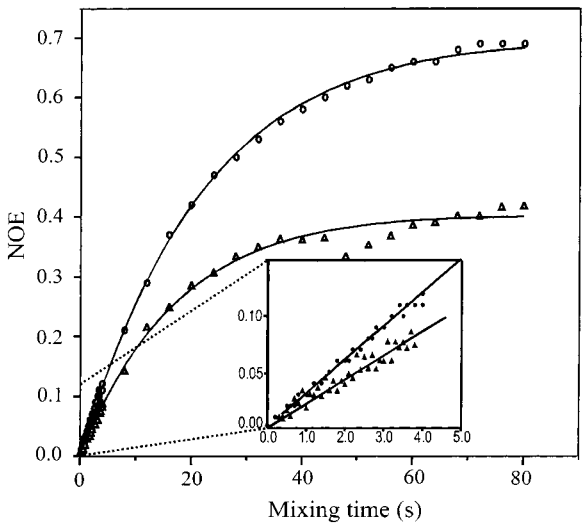

Figure 2. ^1H, ^6Li HOE buildup curves of **1***LiCN (△) and **1** (○), both 0.72 M in Et_2O at 239 K. The initial linear buildup region is enlarged.

To elucidate the structure of organolithium compounds in solution ^1H, ^6Li HOESY experiments are commonly used.[5,12] In most of the quantitative studies involving assessment of H−Li distances for compounds such as **1***LiCN and **1**, HOESY or 1D HOE buildup rates are used.

The 1D ^1H, ^6Li HOE buildup curves of **1***LiCN and **1** in Et_2O recorded at 239 K are shown in Figure 2. The analysis of Figure 2 shows small difference in the slopes of the initial buildups (σ) and a large difference in the maximum enhancement values (η_{max}) for **1***LiCN and **1**. For the quantification of HOESY or 1D HOE buildup rates, distance calculations are usually based on known distances within the molecule. In the case of **1***LiCN and **1** only one ^1H, ^6Li HOE can be observed due to the symmetry of these compounds. This means that there is no distance that could be used as a reference for the calculation of H−Li distances. Therefore, the different correlation times (τ_c) of **1***LiCN and **1** have to be determined to calculate H−Li distances.

Several approaches can be used for the calculation of the motional correlation time τ_c.[13] These are, for example, (1) ^{13}C spin−lattice relaxation time (T_1) measurements, (2) ^1H, ^{13}C HOE initial buildup rate measurements, and (3) measurements of ^1H, ^6Li HOE maximum values. In our study, due to the permanent fast rotation of the methyl groups, methods 1 and 2 can yield only the local τ_c, reflecting mainly the internal rotation of the methyl groups. In the extreme narrowing limit the τ_c values obtained from these methods can be used as a first approximation for the effective motional correlation time of the molecule.[14] However, the weak negative ^1H, ^1H NOEs observed for **1***LiCN and **1** (see section SYM-BREAK-NOE/ROE-HSQC Studies) indicate that these molecules are on the slow tumbling side near the crossover point of the NOE enhancement ($\omega\tau_c = 1.12$). Therefore, the extreme narrowing approximation is not valid

(8) Huang, H.; Liang, C. H.; Penner-Hahn, J. E. *Angew. Chem.* **1998**, *110*, 1628−1630; *Angew. Chem., Int. Ed. Engl.* **1998**, *37*, 1564−1567.

(9) Huang, H.; Alveraz, K.; Liu, Q.; Barnhart, T. M.; Snyder, J. P.; Penner-Hahn, J. E. *J. Am. Chem. Soc.* **1996**, *118*, 8808−8816.

(10) Bertz, S. H.; Nilsson, K.; Davidsson, Ö.; Snyder, J. P. *Angew. Chem.* **1998**, *110*, 327−331; *Angew. Chem., Int. Ed. Engl.* **1998**, *37*, 314−317.

(11) Gschwind, R. M.; Rajamohanan, P. R.; Xie, X. Submitted for publication.

(12) (a) Bauer, W.; Müller, G.; Pi, R.; Schleyer, P. v. R. *Angew. Chem.* **1986**, *98*, 1130−1132; *Angew. Chem., Int. Ed. Engl.* **1986**, *25*, 1103−1105. (b) Bauer, W.; Clark, T.; Schleyer, P. v. R. *J. Am. Chem. Soc.* **1987**, *109*, 970−977. (c) Review: Bauer, W.; Clark, T.; Schleyer, P. v. R. *Adv. Carbanion Chem.* **1992**, *1*, 89−175. (d) Review: Mo, H.; Pochapsky, T. C. *Prog. NMR Spectrosc.* **1997**, *30*, 1−38. (e) Hilmersson, G.; Arvidsson, P. I.; Davidsson, O.; Hakansson, M. *J. Am. Chem. Soc.* **1998**, *120*, 8143−8149.

(13) Neuhaus, D.; Williamson M. *The Nuclear Overhauser Effect in Structural and Conformational Analysis*; VCH Publishers: New York, 1989; pp 31−32.

(14) Breitmaier, E.; Spohn, K. H.; Berger, S. *Angew. Chem.* **1975**, *87*, 152−168; *Angew. Chem., Int. Ed. Engl.* **1975**, *14*, 144−159.

Table 1. Average H−Li Distances (r_{H-Li}) Calculated from Initial Rates of ^1H, ^6Li HOE Buildup Curves and τ_c Values

	Me_2CuLi*LiCN	(**1***LiCN)	Me_2CuLi (**1**)
no. of H	6	3	6
r_{H-Li} (pm)	242 ± 9^a	215 ± 4^a	243 ± 3^a

[a] Experimental error range.

and methods 1 and 2 are not applicable to our systems. It thus turns out that the use of the ^1H, ^6Li HOE maximum value for the determination of τ_c (method 3) is the most appropriate approach in this case, since in the region around the crossover point the effect of the leakage term becomes almost negligible, and η_{max} depends mostly on the resonance frequency and on τ_c.[15] With method 3 the values obtained for τ_c are on the order of 1.6 and 1.0 ns for **1***LiCN and **1**, respectively. (A detailed description of the calculation method of τ_c is given in the Supporting Information.) Due to the fact that the correlation times calculated for **1***LiCN and **1** are in the region around the crossover point, the σ and η_{max} parameters are very sensitive to τ_c. That means that the different values observed for these two parameters are not necessarily due to different H−Li distances.

The average H−Li distances r_{H-Li} for **1***LiCN and **1**, calculated with the τ_c values estimated by the use of method 3, are shown in Table 1. It has been shown previously[3c,h,4d,f,g,i,7] that the salt-free compound **1** has a homodimeric structure **I** (Figure 1), in which each Li^+ is surrounded by 6 protons (two methyl groups) closer than 400 pm. Consequently, the distance r_{H-Li} is to be calculated with 6 protons, resulting in a distance r_{H-Li} of 243 ± 3 pm. (The experimental data and the calculation of r_{H-Li} are given in the Supporting Information.) In the case of **1***LiCN the calculation with 6 protons gives nearly the same value (r_{H-Li} of 242 ± 9 pm). The essentially identical results indicate a similar core structure for **1***LiCN and **1** (the homodimeric structure **I**) in Et_2O. For **1***LiCN in the form of the heterodimer **II**, the protons of only one methyl group would contribute to the ^1H, ^6Li HOE (Figure 1). This results in a shorter r_{H-Li} distance, namely 215 ± 4 pm. Is the similarity between the distances r_{H-Li}, calculated with 6 protons (Table 1) for **1***LiCN and **1**, purely coincidental or does it indicate a homodimeric structure **I** in both cases? To answer this question the NMR results were compared with known structural data.

Since a heterodimeric crystal structure of the type **II** has never been obtained, the only available data of this structural type are those of ab initio calculations.[4c,d,16] Driven by the fact that H−Li distances are not listed in these publications, the trend in the H−Li distances derived from NMR with 3 and 6 protons was interpreted on the basis of the C−Li distances obtained from the ab initio calculations. Ab initio calculations performed for homodimeric (**I**) and heterodimeric structures (**II**) of iodocuprate **1***LiI[4d] and cyanocuprate **1***LiCN[4c,16] are available for this comparison. The structures of the solvated molecules $\mathbf{I_s}$, $\mathbf{II_{s(I)}}$, and $\mathbf{II_{s(CN)}}$, used for the ab initio calculations, are shown in Figure 3. The nonsolvated dimeric structures of **1***LiCN and **1**, corresponding to **I** and **II**, are shown in Figure 1. The C−Li distances calculated for the structures **I**, **II**, $\mathbf{I_s}$, $\mathbf{II_{s(I)}}$, and $\mathbf{II_{s(CN)}}$ are listed in Table 2.

In the case of the solvated **1***LiI and the nonsolvated **1***LiCN the ab initio calculations provided rather similar r_{C-Li} values for both hetero- and homodimers: r_{C-Li} calculated for the solvated **1***LiI ($\mathbf{II_{s(I)}}$) amounts to 219 pm and for **1***LiI ($\mathbf{I_s}$) to 222 pm (Table 2). The nonsolvated **1***LiCN (**II**) and **1***LiCN (**I**) yielded r_{C-Li} values of 207 and 204 pm, respectively. These values imply that there are no significant differences in the r_{C-Li} values between homo- and heterodimeric structures of the solvated **1***LiI and the nonsolvated **1***LiCN. In contrast, assuming that a heterodimer exists in solution, the NMR results require a shorter r_{H-Li} value for the heterodimer (215 pm) than the homodimer (242 pm). Thus, the analysis of the values for **I**, **II**, $\mathbf{I_s}$, and $\mathbf{II_{s(I)}}$ (Table 2) and the NMR results (Table 1) lead to the conclusion that **1***LiCN exists in the form of a homodimer **I** in Et_2O. Only in the case of the solvated **1***LiCN does the heterodimer $\mathbf{II_{s(CN)}}$ show a slightly shorter distance r_{C-Li} (212 pm) than the homodimer $\mathbf{I_s}$ (225 pm, Table 2). Therefore, further studies were performed to obtain additional structural information for the differentiation between the heterodimer **II** and the homodimer **I** in the case of **1***LiCN in Et_2O.

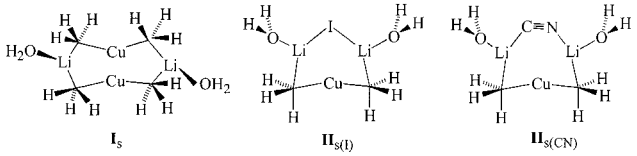

Figure 3. Structures of solvated (s) **1** (homodimer $\mathbf{I_s}$),[4d,16] **1***LiI (heterodimer $\mathbf{II_{s(I)}}$),[4d] and **1***LiCN (heterodimer $\mathbf{II_{s(CN)}}$)[4c,16] from ab initio calculations.

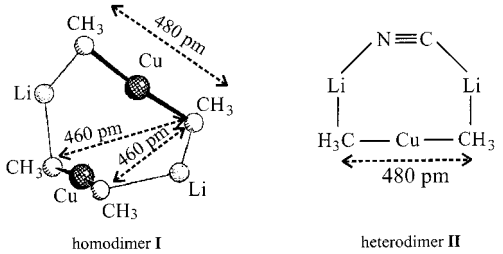

Figure 4. Differentiation between the structural motifs of **1***LiCN as a homodimer **I** or a heterodimer **II** by ^1H, ^1H NOE. The attached numbers refer to the average proton−proton distances between the methyl groups. See text for details.

Table 2. Average C−Li Distances (pm) by ab Initio Calculations

	Me_2CuLi*LiI[4d] (**1***LiI)	Me_2CuLi*LiCN[4c,16] (**1***LiCN)	
	solv.(H_2O)	non-solv.	solv.(H_2O)
heterodimer	219 ($\mathbf{II_{s(I)}}$)	207 (**II**)	212 ($\mathbf{II_{s(CN)}}$)
homodimer	222 ($\mathbf{I_s}$)	204 (**I**)	225 ($\mathbf{I_s}$)

SYM-BREAK-NOE/ROE-HSQC Studies. Investigations of the $^1H-^1H$ dipolar interactions can be an alternative method of elucidating structural information for **1***LiCN and **1** in Et_2O. Homodimer **I** and heterodimer **II** have different numbers of protons contributing to the NOE signals and slightly different distances between the protons. In homodimer **I** each methyl group is surrounded by 3 other methyl groups, contributing to its ^1H, ^1H NOE intensity; in the heterodimeric structure **II** only 1 methyl group contributes to the $^1H-^1H$ dipolar interaction (Figure 4). Consequently, in the case of a homodimeric structure of **1***LiCN, the ^1H, ^1H NOE intensities of **1***LiCN and **1** should be similar, whereas for a heterodimeric structure of **1***LiCN, the ^1H, ^1H NOE intensities should be rather different. Therefore ^1H, ^1H NOE experiments should serve as a powerful tool for the structure determination of **1***LiCN in Et_2O.

Due to the symmetry of **1***LiCN and **1** the only observable $^1H-^1H$ dipolar interaction is the one between chemically equivalent methyl groups. Since the common experiments for

(15) Neuhaus, D.; Williamson M. *The Nuclear Overhauser Effect in Structueal and Conformational Analysis*; VCH Publishers: New York, 1989; pp 46−55.

(16) Böhme, M. Quantenmechanische Berechnungen von Kupfer-(I)-Verbindungen, Ph.D. Thesis, Fachbereich Chemie, Philipps-Universität Marburg, 1993.

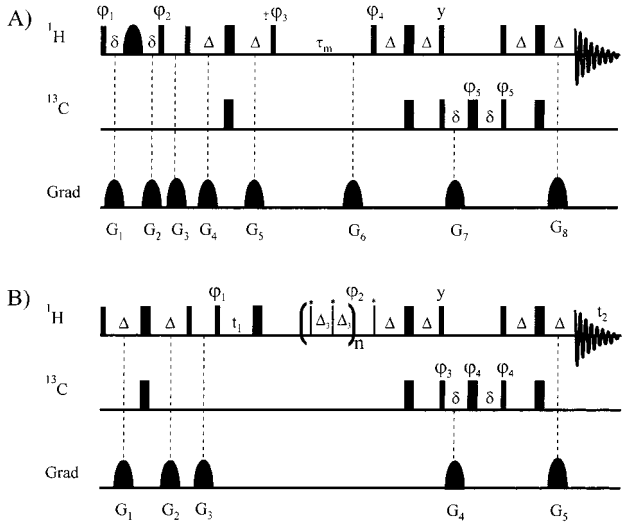

Figure 5. Pulse sequences for (A) selective 1D SYM-BREAK-NOE-HSQC and (B) 2D SYM-BREAK-ROE-HSQC experiments. All 90° (180°) pulses are represented by narrow (wide) rectangles and the Gaussian cascades (G3) selective pulse[24] by a solid sine-bell. Low flip angle pulses are denoted with asterisks. All pulses have phase *x* unless indicated otherwise. In part B, quadrature detection in F_1 was achieved by States-TPPI cycling of phase φ_1.[26] The delay settings are as follows: $\Delta = 1/(4*^1J_{CH})$, $\delta = 1.5$ ms, τ_m= mixing time, $\Delta_3 = 3$ μs (delay for pulsed spin-lock). The gradient strengths (*z* direction) are as follows: (A) $G_1 = 20$, $G_2 = 20$, $G_3 = 40$, $G_4 = 10$, $G_5 = 10$, $G_6 = 90$, $G_7 = 79.5$, $G_8 = 20$; (B) $G_1 = 10$, $G_2 = 10$, $G_3 = 90$, $G_4 = 79.5$, $G_5 = 20$. The phase cycle is the following: (A) $\varphi_1 = 8(x)$, $8(-x)$; $\varphi_2 = 2(x)$, $2(-x)$; $\varphi_3 = 2(x)$, $2(-x)$, $2(x)$, $4(-x)$, $2(x)$, $2(-x)$, $2(x)$; $\varphi_4 = x$, $-x$; $\varphi_5 = 4(x)$, $4(-x)$; $\varphi_{rec} = x, -x, x, 2(-x), x, -x, 2(x), -x, x, 2(-x), x, -x, x$; (B) $\varphi_1 = 2(x)$, $2(-x)$; $\varphi_2 = 2(y)$, $2(-y)$; $\varphi_3 = x, -x$; $\varphi_4 = 4(x)$, $4(-x)$; $\varphi_{rec} = x, 2(-x), x, -x, 2(x), -x$.

this purpose, the HMQC-ROESY[17a] and HSQC-NOESY,[17b] were found to be too insensitive to observe these interactions, we had to develop a new pulse sequence. Thus, the SYM-BREAK-NOE/ROE-HSQC experiments were introduced to observe NOEs between equivalent protons positioned at large distances.[11] The SYM-BREAK-NOE/ROE-HSQC experiments are tailored to the different relaxation properties of the ^{1}H−^{13}C and ^{1}H−^{12}C isotopomers. For protons directly attached to ^{13}C, the strong dipolar interaction between the proton and the carbon is the main relaxation source for long proton−proton distances and reduces the detected NOE/ROE. For example, at the average proton−proton distance of 480 pm in one monomeric unit of **1** the relative cross-relaxation rate for the ^{1}H, ^{1}H NOEs is lower than 5%. However, for protons directly attached to ^{12}C, the proton−proton dipolar interaction is still dominant, and the relative cross-relaxation rate for the ^{1}H, ^{1}H NOEs remains higher than 95%.[11]

Therefore, in the pulse sequences of the SYM-BREAK-NOE/ROE-HSQC experiments, we started from protons directly attached to ^{12}C. The corresponding isotope filter is then followed by a NOE/ROE transfer and a selection of the protons attached to ^{13}C (for a detailed description see ref 11). This approach leads to large sensitivity enhancement for long-range NOEs between equivalent protons and allows for detection of ^{1}H−^{1}H dipolar interactions in **1***LiCN and **1**.

The pulse sequences of the selective 1D SYM-BREAK-NOE-HSQC and the 2D SYM-BREAK-ROE-HSQC experiments are shown in Figure 5. In the 1D experiment, the NOE buildup

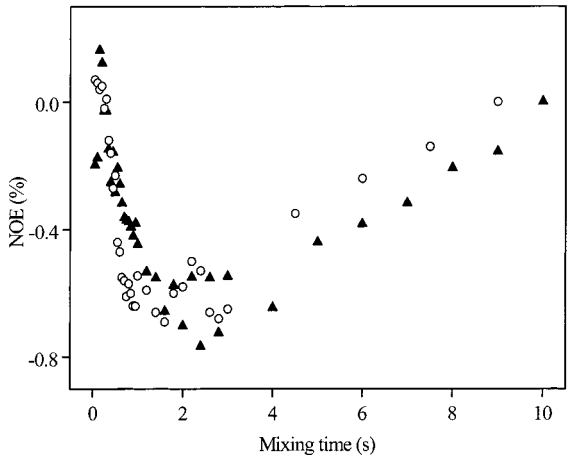

Figure 6. ^{1}H, ^{1}H SYM-BREAK-NOE-HSQC buildup curves of [20% ^{13}C]-labeled **1***LiCN (○) and **1** (▲), both 0.72 M in Et_2O at 239 K.

curves were obtained similarly to standard NOE difference spectroscopy. Thus, two spectra were recorded using a phase change of the proton 90° pulse prior to the mixing period from φ_3 to $-\varphi_3$ (Figure 5A). The first experiment gives only the relaxation component without NOE, while the second shows the relaxation component with NOE. The difference between these two spectra gives the relative NOE enhancement. The 2D SYM-BREAK-ROE-HSQC experiment (Figure 5B) has been designed for the detection of ROEs between equivalent protons in symmetrical molecules with τ_c values near the crossover point of the NOE enhancement. The pulse sequence of the 2D SYM-BREAK-ROE-HSQC is similar to that of the 2D SYM-BREAK-NOE-HSQC,[11] except that the NOE transfer is replaced by a ROE transfer. The resulting 2D SYM-BREAK-ROE-HSQC spectrum is similar to a 2D ^{1}H, ^{1}H ROESY spectrum,[18] with the cross-peaks split into a doublet by the $^1J_{HC}$ coupling in the direct dimension. The strong diagonal peaks are suppressed by the two X-filters. Hence, the sensitivity of the receiver can be adjusted to the small cross-peak intensities. This allows an additional signal-to-noise ratio improvement.

The selective 1D SYM-BREAK-NOE-HSQC experiment was applied to [20% ^{13}C]-labeled samples of **1***LiCN and **1** (0.72 M in Et_2O), and the corresponding NOE buildup curves are shown in Figure 6. It can be seen that both compounds exhibit a weak negative NOE, with a similar slope in the initial buildup region, and a slight deviation in the later part, where relaxation occurs. Does this obvious similarity in the ^{1}H, ^{1}H NOE intensities of **1***LiCN and **1** indicate identical structures? For a clear answer, the interproton distances from already known structures of the homodimer type **I** have to be compared with those of a heterodimer **II**.

The ab initio calculations for **1***LiCN and **1** performed without and with two water molecules exhibit a solvent dependence of the Li−C distances and of the torsion angle between the two Me−Cu−Me units.[4c,16] Since there exist no calculations for **1***LiCN and **1** in Et_2O, crystallographic data of a similar system had to be used for the calculation of the expected ^{1}H, ^{1}H NOE enhancement. Fortunately, the crystal structure of $((Me_3SiCH_2)_2CuLi)_2*3Et_2O$,[3h] showing a homodimeric structure in Et_2O, could be taken for this purpose. This compound is a Me_3Si derivative of **1** and can therefore be used as a model system. The positions of the protons could not be established directly from the X-ray crystal structure. Therefore

(17) (a) Kawabata, J.; Fukushi, E.; Mizutani, J. *J. Am. Chem. Soc.* **1992**, *114*, 1115−1117. (b) Wagner, R.; Berger, S. *Magn. Reson. Chem.* **1997**, *35*, 199−202.

(18) (a) Bothner-By, A. A.; Stephens, R. L.; Lee, J.; Warren, C. D.; Jeanloz, R. W. *J. Am. Chem. Soc.* **1984**, *106*, 811−813. (b) Bax, A.; Davis, D. J. *J. Magn. Reson.* **1985**, *63*, 207−213.

they were calculated by using the Add Hydrogens procedure of HyperChem[19] (Me_3Si groups were replaced by protons). In the case of the heterodimeric structure, the H−H distances within the heterodimer **II** were assumed to be identical with the H−H distances within one monomeric unit of the homodimer **I**. The average proton−proton distances between the methyl groups are shown in Figure 4.

In addition to the different numbers of protons and different distances, the fast rotation of the methyl groups has to be taken into account. It has been shown that for fast internal rotations involving distance variations the cross-relaxation rate, which is correlated with the ^{1}H, ^{1}H NOE, is proportional to $\langle r^{-3}\rangle^2$.[20] For this special averaging the individual proton−proton distances derived from the crystal structure of $((Me_3SiCH_2)_2CuLi)_2$*$3Et_2O$[3h] were used. Accordingly, the presence of the heterodimeric structure **II** would lead to only 23% of the NOE intensity of the homodimeric structure **I**. Therefore, the similar slope in the initial buildup region of the ^{1}H, ^{1}H NOE obtained for **1***LiCN and **1** in Et_2O can be explained only by a homodimeric core structure **I** of both compounds **1***LiCN and **1**. The slight deviation in the later part, where relaxation occurs, can be explained by the slight differences in τ_c and the different relaxation properties of these two samples.

The NOE expected for a dimeric structure **I** should be positive under the experimental conditions used, rather than negative as observed (Figure 6). This is confirmed by three test experiments performed on two systems with known structures. Thus Me_2S in THF was used as a monomer-model, and $(Me_3SiCH_2)_2CuLi$ in Et_2O as a model for a dimer. The SYM-BREAK-NOE-HSQC buildup curves of Me_2S (1 M, natural abundance) showed indeed a positive NOE at 273 and 239 K. Standard ^{1}H, ^{1}H NOESY of $(Me_3SiCH_2)_2CuLi$ in Et_2O (0.67 M, natural abundance) at 239 K showed negative cross-peaks also indicating a positive NOE. A possible explanation for the negative sign of the NOEs observed for **1***LiCN and **1** is the formation of aggregates higher than a dimer. The formation of aggregates of organocuprates in Et_2O was already indicated in previous publications. Thus, much more complex ^{15}N NMR spectra in Et_2O than THF were observed for Bu_2CuLi*LiCN,[10] and the presence of higher aggregates of heterocuprates in Et_2O was recently confirmed by electrospray ionization mass spectrometry.[21]

The change in the sign of the NOE from positive to negative, which is observed in this work, was also reported for tetraalkylammonium tetrahydroborates in $CDCl_3$, and was explained there by the formation of multiion aggregation at low temperatures.[22] Furthermore, the sign and the magnitude of the NOE were found to be independent of the concentration of the samples. An experiment performed on **1***LiCN at a lower concentration (0.36 M in Et_2O) shows no significant concentration dependence of the NOE intensities. Therefore, we assume also higher aggregates for **1***LiCN and **1**. This is in agreement with solid-state investigations, in which polymeric chains are typical structures of organocuprates.[3c,f,g] For example, in the crystal structure of $[Li_2Cu_2(CH_2SiMe_3)_4(SMe_2)_2]_\infty$,[3c] homodimeric core structures **I**, similar to that of **1**, are linked to each other by solvent molecules SMe_2. Second, the heterocuprate $[t$BuCu(CN)$Li(OEt_2)_2]_\infty$ exists as a chain of homodimers being bridged by solvated Li^+ ions.[3g] An example of the participation of CN^- anions is shown in the crystal structure of the linear polymeric $[(2\text{-}(Me_2NCH_2)C_6H_4)_2CuLi_2(CN)(THF)_4]_\infty$,[3f] with Li^+ cations being bridged by CN^- anions. Therefore, the most probable explanation for the observed negative NOEs is that **1***LiCN and **1** tend to form linear chains of homodimers **I** as suggested by the crystal structures. In such a case, additional proton−proton interactions between the different homodimeric core structures **I** have to be considered. The experimental data closest to our system are those obtained from the crystal structure of $[Li_2Cu_2(CH_2SiMe_3)_4(SMe_2)_2]_\infty$. With the additional proton−proton interactions elucidated for distances lower than 550 pm the expected relative NOE intensity of the heterodimer **II** changes slightly from 23% to 25% of that of the homodimer **I**. This change in the NOE intensities is insignificant and does not affect our conclusion of the presence of a homodimeric structure **I** of **1***LiCN in Et_2O.

The higher aggregates of **1***LiCN and **1**, which result in a motional correlation time near the crossover point of the maximum NOE (τ_c in the order of nanoseconds), lead to only small negative NOE enhancements as can be observed in Figure 6. One common way of overcoming this problem, as well as the dependence of the NOE enhancement on the slightly different τ_c values of **1***LiCN and **1**, is the application of the ROE technique.[18] Therefore, a 2D SYM-BREAK-ROE-HSQC experiment was applied to **1***LiCN and **1** under the same experimental conditions as for the SYM-BREAK-NOE-HSQC (for spectra see Figure S2 in the Supporting Information). Using a mixing time of 300 ms, which is still in the initial linear buildup region, the volume integral for **1***LiCN is 128% of the value for **1**, with a relative experimental error of ±6% (estimated by three repetitions of the measurement). Considering the fact that a heterodimeric core structure **II** of **1***LiCN would produce only 25% intensity of the value of **1**, the observed ROE intensities similarly indicate the presence of a homodimeric core structure **I** (Figure 4) for **1***LiCN. Slightly different H−H distances (on the order of 4%) for the homodimeric core structures **I** in both compounds might explain the difference in the ROE intensities. Thus, the results of the SYM-BREAK-ROE-HSQC experiments support the existence of a homodimeric core structure **I** for both **1***LiCN and **1** in Et_2O.

Conclusion

The development of the pulse sequences ^{1}H, ^{1}H SYM-BREAK-NOE-HSQC and ^{1}H, ^{1}H SYM-BREAK-ROE-HSQC enables the detection of long-range dipolar interactions between equivalent protons in symmetric systems. In the case of the organocuprates **1***LiCN and **1** in Et_2O, the significant sensitivity enhancements with these pulse sequences allowed for the elucidation of reliable structural information. Thus, similar ^{1}H−^{1}H dipolar interactions were observed for **1***LiCN and **1** in Et_2O, which indicate the presence of a homodimeric core structure **I** for both compounds. Furthermore, the H−Li distances resulting from ^{1}H, ^{6}Li HOE buildup curves are in agreement with a homodimeric structure **I** of **1***LiCN in Et_2O.

These results are in correspondence with a quantum mechanical study of Bertz et al.,[4d] where an equilibrium between homodimeric and heterodimeric structures was proposed for **1***LiI. However, they contradict the general opinion on the structures of salt-containing organocuprates, which have been

(19) *HyperChem*; Hypercube, Inc.: 1115 NW 4th Street, Gainesville, FL 32601.

(20) (a) Tropp, J. *J. Chem. Phys.* **1980**, *72*, 6035−6043. (b) Keepers, J. W.; James, T. L. *J. Magn. Reson.* **1984**, *57*, 404−426. (c) Pegg D. T.; Bendall, M. R.; Doddrell, D. M. *Aust. J. Chem.* **1980**, *33*, 1167−1173. (d) Neuhaus, D.; Williamson M. *The Nuclear Overhauser Effect in Structural and Conformational Analysis*; VCH Publishers: New York, 1989; pp 174−175.

(21) Lipshutz, B. H.; Keith, J.; Buzard, D. J. *Organometallics* **1999**, *18*, 1571−1574.

(22) (a) Pochapsky, T.; Stone, P. M. *J. Am. Chem. Soc.* **1990**, *112*, 6714−6715. (b) Stone, P. M.; Pochapsky, T. C.; Callegari, E. *J. Chem. Soc., Chem. Commun.* **1992**, 178−179. (c) Pochapsky, T. C.; Wang, A. P.; Stone, P. M. *J. Am. Chem. Soc.* **1993**, *115*, 11084−11091.

modeled on the basis of a number of theoretical calculations and EXAFS studies.

Previously it has been shown that in the reactions of organocuprates with enones in solution the CIPs are the reactive species.[3h] In this context our results clearly show that for **1***LiCN and **1** in Et_2O the structure of the CIPs is not strongly affected by the presence of the salt. This implies that even for salt-containing organocuprates a homodimeric structure **I** is expected to be the reactive species in the reaction with enones.

Experimental Section

Sample Preparation. Compound **1** was prepared by a method described by Bertz et al.[4d] and John et al.[3h] [^{13}C]-labeled MeLi was prepared by reacting [^{13}C]-labeled MeI with *n*-BuLi. Subsequently, CuI was reacted with [20% ^{13}C]-labeled MeLi in dry Et_2O at 233 K to obtain Me_2CuLi*LiI, which was then reacted with 2-cyclohexenone at 195 K without isolation. The reaction mixture was centrifuged for 5 min at 195 K to separate the yellow solid MeCu, which was then washed with dry Et_2O and reacted with ^{6}Li-enriched MeLi to obtain **1**. **1***LiCN was prepared by reacting CuCN with ^{6}Li-enriched and [20% ^{13}C]-labeled MeLi in dry Et_2O at 233 K under argon atmosphere. The solvent was then evaporated at 273 K under vacuum until a clear oil remained which was redissolved in Et_2O-d_{10} and transferred into a NMR tube. The samples were kept at 195 K and were found to be stable at this temperature for more than 8 weeks. $(Me_3SiCH_2)_2CuLi$ in Et_2O was prepared following the method described by John et al.[3h]

NMR Instrumental Procedure. The NMR spectra were recorded on Bruker DRX500 and DRX400 spectrometers equipped with a 5 mm broadband triple resonance gradient probe. The DRX500 was used to measure ^{1}H, ^{6}Li HOE, ^{1}H, ^{13}C HOE, and ^{1}H, ^{1}H NOE buildup curves with resonance frequencies of 500.13, 125.76, and 73.7 MHz for ^{1}H, ^{13}C, and ^{6}Li, respectively. The DRX400 was used to measure the ^{1}H, ^{1}H ROE with a resonance frequency of 400.13 MHz. The proton and carbon spectra were referenced to external TMS, and the ^{6}Li spectra to a 1 M solution of LiCl in water ($\delta = 0$ ppm) at 273 K. Typical 90° pulses were equal to 14, 11, and 13 μs for ^{1}H, ^{13}C, and ^{6}Li, respectively. All measurements were carried out at 239 K unless indicated otherwise. The temperature was controlled by a Bruker BVT 3000 unit.

NMR DATA Collection and Processing. Samples with [^{6}Li]-labeling were used at a concentration of 0.72 M. The concentrations of the samples were precisely adjusted by comparing the integral of the proton spectra obtained by a single 90° pulse. Experiments for 1D NOE and HOE buildup curves were carried out similarly to standard NOE difference spectroscopy. For the normalization of the spectra at different mixing times, one spectrum of $\tau_m \geq 5T_1$ without HOE was used.

In the ^{1}H, ^{6}Li HOE experiments, the cuprate protons were selectively saturated by a string of long low power pulses. For each buildup curve 80 points were collected with mixing times up to 80 s. The initial part consisted of 40 points, with a 100 ms increment in the mixing time up to 4 s. For the remaining part of the buildup curve an increment of 4 s was used. One scan was applied to each increment with 250 s relaxation delay.

In the ^{1}H, ^{13}C HOE experiments the same samples as for ^{1}H, ^{6}Li HOE experiments were used. The protons were saturated using Waltz-16 composite pulse decoupling.[23] For each buildup curve 50 points were collected with mixing times up to 6 s. The initial part consisted of 40 points, with a 25 ms increment in the mixing time up to 1 s. For the later part an increment of 0.5 s was used. For each increment 16 scans were applied with 20 s relaxation delay.

In the selective 1D SYM-BREAK-NOE-HSQC experiments a Gaussian cascades (G3) selective pulse (20 ms) was used.[24] The samples used were with additional [20% ^{13}C]-labeling. For the buildup curve of **1**, 47 points were collected with mixing times up to 10 s, and 43 points for that of **1***LiCN with mixing times up to 9 s. For both samples 32 scans were used for each increment with 10 s relaxation time. The delay Δ of the isotope filter was adjusted from 2.29 to 2.28 ms, which corresponds to an adjustment in the coupling constant J_{CH} from its actual value of 109.5 Hz to 109.0 Hz to compensate for the artifacts of the anti-phase term not completely suppressed by the isotope filter. The typical experimental time required for a buildup curve was about 12 h.

In the 2D SYM-BREAK-ROE-HSQC experiments the same samples as for the 1D SYM-BREAK-NOE-HSQC experiments were used. Low flip angle transmitter pulses were applied for spin-lock.[25] The parameters were chosen as follows: spectral window of 8 ppm for both dimensions ($F_1 = F_2 = {}^1$H); 8192 points in the F_2 dimension, 512 increments and 16 scans for each increment, mixing time 300 ms, and 5 s relaxation delay. The pulse length of the low flip angle spin-lock pulses was 2 μs and the spin-lock power 4 kHz. The typical experimental time was about 13 h. The data were processed with the software package X-WINNMR (Bruker). Apodization with a square sine bell weighting in F_1 and exponential multiplication with a line broadening of 2 Hz in F_2 was applied. Quadrature detection in the indirect dimension was achieved by TPPI.[26]

Acknowledgment. We gratefully acknowledge financial support from the Deutsche Forschungsgemeinschaft (Sonderforschungsbereich 260) and the Fonds der Chemischen Industrie.

Supporting Information Available: Calculations of the τ_c values and H−Li distances, and SYM-BREAK-ROE-HSQC spectra of **1***LiCN and **1** (PDF). This material is available free of charge via the Internet at http://pubs.acs.org.

JA004350X

(23) Shaka, A. J.; Keeler, J.; Freeman, R. *J. Magn. Reson.* **1983**, *53*, 313−340.

(24) (a) Emsley, L.; Bodenhausen, G. *J. Magn. Reson*. **1989**, *82*, 211−221. (b) Emsley, L.; Bodenhausen, G. *Chem. Phys. Lett*. **1990**, *165*, 469−476.

(25) Kessler, H.; Griesinger, C.; Kerssebaum, R.; Wagner, K.; Ernst, R. R. J. *Am. Chem. Soc*. **1987**, *109*, 607−609.

(26) Marion, D.; Ikura, M.; Tschudin, R.; Bax, A. *J. Magn. Reson*. **1989**, *85*, 393−399.